

Prograde infiltration of Cl-rich fluid into the granulitic continental crust from a collision zone in Perlebandet, Sør Rondane Mountains, East Antarctica

*河上 哲生¹、東野 文子^{1,2}、Skrzypek Etienne¹、Satish-Kumar Madhusoodhan³、Grantham Geoffrey⁴、土屋 範芳²、石川 正弘⁵、坂田 周平^{1,6}、平田 岳史^{1,7}

*Tetsuo Kawakami¹, Fumiko Higashino^{1,2}, Etienne Skrzypek¹, Madhusoodhan Satish-Kumar³, Geoffrey Hugo Grantham⁴, Noriyoshi Tsuchiya², Masahiro Ishikawa⁵, Shuhei Sakata^{1,6}, Takafumi Hirata^{1,7}

1. 京都大学、2. 東北大学、3. 新潟大学、4. ヨハネスブルグ大学、5. 横浜国立大学、6. 学習院大学、7. 東京大学

1. Kyoto Univ., 2. Tohoku Univ., 3. Niigata Univ., 4. Univ. of Johannesburg, 5. Yokohama National Univ., 6. Gakushuin Univ., 7. Univ. Tokyo

Timing of Cl-rich fluid infiltration is correlated with the pressure-temperature-time (*P-T-t*) path of upper amphibolite- to granulite-facies metamorphic rocks utilizing microstructures of Cl-bearing biotite in pelitic and felsic metamorphic rock from the continental collision zone (Perlebandet, Sør Rondane Mountains (SRM), East Antarctica). Microstructural observation indicates that the stable Al₂SiO₅ polymorph changed from sillimanite to kyanite + andalusite + sillimanite, and *P-T* estimates from geothermobarometry point to a counterclockwise *P-T* path characteristic of the SW terrane of the SRM (e.g., Osanai et al., 2013) *In situ* LA-ICPMS U-Pb dating of zircon inclusions in garnet yielded ca. 580 Ma, likely representing the age of garnet-forming metamorphism at Perlebandet.

Inclusion-host relationships among garnet, sillimanite, and Cl-rich biotite (Cl > 0.4 wt%) reveal that formation of Cl-rich biotite took place during prograde metamorphism in the sillimanite stability field. This process probably predated partial melting consuming biotite (Cl = 0.1-0.3 wt%). This was followed by retrograde, moderately Cl-bearing biotite (Cl = 0.1-0.3 wt%) replacing garnet. Similar timings of Cl-rich biotite formation in different samples, and similar $f(\text{H}_2\text{O})/f(\text{HCl})$ values of coexisting fluid estimated for each stage can be best explained by Cl-rich fluid infiltration during prograde metamorphism.

Fluid-present partial melting at the onset of prograde metamorphism probably contributed to elevate Cl concentration (and possibly salinity) of the fluid, and consumption of the fluid resulted in the progress of dehydration melting. The retrograde fluid was released from crystallizing Cl-bearing partial melts or derived externally.

The prograde Cl-rich fluid infiltration in Perlebandet presumably took place at the uppermost part of the footwall of the collision boundary. Localized distribution of Cl-rich biotite and hornblende along large-scale shear zones and detachments in the SRM (Higashino et al., 2013; 2015) supports external input of Cl-rich fluids through tectonic boundaries during continental collision.

キーワード：流体、変成作用、部分溶融、塩素、大陸衝突

Keywords: Fluid, Metamorphism, Partial melting, Chlorine, Continental collision

東南極リュツォ・ホルム岩体明るい岬に産するコランダム周囲に発達する コロナの形成: 反応の律速過程と温度圧力勾配

Formation of Corona around Corundum from Akarui Point in the Lützow-Holm Complex, East Antarctica: Controlling factor and P-T slope of reaction

*森 祐紀¹、池田 剛²

*Yuki Mori¹, Takeshi Ikeda²

1. 九州大学大学院理学府地球惑星科学専攻、2. 九州大学大学院理学研究院地球惑星科学部門

1. Department of Earth and Planetary Sciences, Graduate School of Sciences, Kyushu University, 2. Department of Earth and Planetary Sciences, Faculty of Sciences, Kyushu University

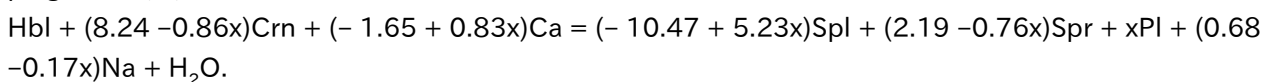
Corona, a disequilibrium texture, is often found in metamorphic rocks. Its textural feature that preserves both reactant and product minerals gives us various information for metamorphic reactions including mass transfer, diffusion and pressure (P) –temperature (T) path. In this study, we dealt with a corona developing between corundum and hornblende in ultrabasic gneiss, and revealed controlling factor of zonal arrangement, reaction, volume change and P-T slope of corona formation.

The studied gneiss composed mainly amphibole and plagioclase was collected from Akarui Point in the Lützow-Holm Complex, East Antarctica. Corundum grains in the rock are surrounded by corona composed of green spinel, sapphirine and plagioclase that are regularly arranged from corundum to the matrix. In the matrix, hornblende, plagioclase and gedrite occur together with minor brownish-green spinel, biotite and opaque minerals. The brownish-green spinel also occurs as inclusion in corona plagioclase or at the outer border of corona sapphirine.

Chemical composition of corundum is almost pure Al_2O_3 . Cr content in green spinel is as low as 0.00 –0.01 apfu (O = 4), while brownish-green spinel contains significant amount of Cr as 0.08 –0.26 apfu. Si content of corona sapphirine increases and Al content decreases outward. Anorthite content [$=100 \cdot \text{Ca}/(\text{Ca}+\text{Na})$] of corona plagioclase decreases from inner to outer part (from 89 to 78). Hornblende and gedrite are classified with pargasite and sodicgedrite according to Leake et al. (1997), respectively. $\text{Ca}/(\text{Ca}+\text{Na})$ of hornblende ranges from 0.67 to 0.74.

Al contents of constituent minerals normalized by 40 oxygen decrease in the following order: corundum, spinel, sapphirine, plagioclase and hornblende. Corona sapphirine and plagioclase show a similar feature that Al decreases outward. Si content shows inverse trend to Al in sapphirine and plagioclase, so these features suggest that diffusion of Al and Si controlled corona formation.

Stoichiometric equation of the reaction is estimated by considering mass-balance in the $\text{Na}_2\text{O} - \text{CaO} - \text{MgO} - \text{Al}_2\text{O}_3 - \text{SiO}_2 - \text{H}_2\text{O}$ system. The value of $\text{Ca}/(\text{Ca}+\text{Na})$ differs between hornblende and plagioclase, which requires to treat Na, Ca or both as mobile component. The resultant equations are inconsistent with the microstructure in the case of only one mobile component (Na or Ca). Calculation with treating both Na and Ca as mobile component provides following equations in which stoichiometric coefficient of plagioclase, x, is introduced as a variable.



The microstructure constrained the range of x as 2.00 –2.87. This result suggests that inflow of Ca and outflow of Na occurred during corona formation.

We also estimated volume change and slope in P-T space of the reaction by using standard molar volume

and entropy of Holland and Powell (1998). Total volume and entropy of products are always larger than those of reactant in the range of $2.00 < x < 2.87$. This result means that volume increased by the corona formation and the slope of the reaction is positive. Previous studies (e.g., Iwamura et al. 2013) have revealed that the complex experienced nearly isothermal decompression in a clockwise P-T path. It may be suggested that the corona-forming reaction took place during the decompression.

We conclude the history of the corona formation as bellow. Corundum contacts with hornblende before corona formation at high pressure. The corona-forming reaction that has positive P-T slope was triggered by decompression. The diffusion of Al and Si controlled the rate of mass transfer, during which Ca was supplied and Na was released.

キーワード：コロナ、反応組織、リュツォ・ホルム岩体

Keywords: corona, reaction texture, the Lützow-Holm Complex

Multiply hydration events of pyroxenite and amphibolite in the middle crustal conditions, Sør Rondane Mountains, East Antarctica

*Diana Mindaleva¹, Masaaki Uno¹, Atsushi Okamoto¹, Noriyoshi Tsuchiya¹

1. Graduate School of Environmental Studies, Tohoku University

Fluids in the crust are important for ore deposition, crust evolution and geothermal activity in subduction zones. Fluids supplied from the subducting slab cause hydration reactions, which induce mass and heat transport, redistribution of elements, formation of new minerals, and changes rheology of rocks. The extent, chemistry, time of infiltration, distribution and flow mechanisms mode of such hydration reactions are determined by fluid flow rate, fluid sources and properties of rocks where reaction has happened. Therefore, it is important to understand flow rate and source of fluid for estimating evolution of the Earth's crust in terms of fluid-rock interaction. The main target of this study is estimating of time and conditions of fluid infiltration.

Pyroxenite and amphibolite that is partly hydrated along veins and fractures were collected from Mefiell, Sør Rondane Mountains, East Antarctica during JARE-51 (2009-2010 years). The basement rocks of Sør Rondane Mountains can be divided into amphibolite-facies to granulite-facies Southwestern terrane and granulite-facies to greenschist-facies Northeastern terrane. NE-terrane exhibits a clockwise pressure-temperature-time (P-T-t) path and the SW-terrane exhibits a counter-clockwise P-T-t path (Osanaï et al., 2013). Samples analyzed in this study were collected from SW-terrane.

For pyroxenite, the host rock is dominated by clinopyroxene, orthopyroxene, plagioclase, potassium feldspar with minor amount of ilmenite, apatite and biotite, which are replaced partially by hornblende, biotite, apatite in the veins. Calculated weight percentage of water ranges from 0.1% for host rock to 1.3% as the maximum for the veins.

In the vein, altered clinopyroxene grains are surrounded by hornblende and orthopyroxene grains are surrounded by cummingtonite and actinolite. The X_{Mg} is different between two pyroxenes (X_{Mg} around 0.61 for clinopyroxene in the vein, 0.59 in the host rock and X_{Mg} around 0.48 for orthopyroxene in the vein, 0.46 in the host rock).

In some plagioclase grains cores are represented by albite and rims by anorthite. Anorthite rims boundaries are in contact with tschermakite rims boundaries which surrounding hornblende cores. Conditions estimated by hornblende-plagioclase (Holland and Blundy, 1994), Ti in biotite (Henry et al., 2005) thermometers and Al in hornblende geobarometer (Anderson and Smith, 1995) reveal that P-T conditions of vein formation was estimated to be around 6 kbar and $635\pm 50^\circ\text{C}$ for hornblende and $575\pm 75^\circ\text{C}$ for tschermakite respectively. Contrary, application of two pyroxene thermometer (Wells, 1977) to the host rock shows $850\pm 50^\circ\text{C}$.

These results suggest that hydration of the pyroxenite had occurred through brittle fracture during cooling from granulite-facies to amphibolite-facies under middle crustal condition.

For amphibolite, major minerals are orthopyroxene and amphiboles, with minor amount of ilmenite, anorthite, spinels, muscovite and apatite. In the vein actinolite, serpentine, epidote and magnetite were observed.

Symplectite consists from muscovite and anorthite surrounded by spinels was found along veins. Temperature around $400\pm 50^\circ\text{C}$ was estimated using ilmenite magnetite thermometer (Andersen and Lindsley, 1985) for the veins.

Cl and F were enriched in apatite and micas in the veins.

Foliation parallel veins were formed by hydration events under greenschist-facies to amphibolite-facies, and then foliation vertical veins were occurred in later stage which suggests several infiltration events.

Keywords: hydration, metamorphic rocks

長崎県野母半島の長崎変成岩中の蛇紋岩メランジュの岩石学的研究 Petrological study of the serpentinite melange from the Nagasaki Metamorphic Rocks in the Nomo Peninsula

*外山 茂樹¹、西山 忠男¹

*shigeki toyama¹, Tadao Nishiyama¹

1. 熊本大学

1. kumamoto University

長崎県西彼杵半島、野母半島、熊本県天草下島に分布する結晶片岩類を主体とする低温高圧型の変成岩類は長崎変成岩と呼ばれる。野母半島の長崎変成岩類は、結晶片岩類、蛇紋岩類および変成ハンレイ岩の3つに分類される。蛇紋岩には蛇紋岩メランジュが発達し、蛇紋岩メランジュのマトリクスは、主にアクチノ閃石片岩、緑泥石-アクチノ閃石片岩で構成される。このマトリクスは、非常に片理の発達した剥離性に富む岩石で、レンズ状の岩塊をブロックとして包有している。鉱物組合せは、アクチノ閃石+ホルンブレンド+曹長石+緑泥石+緑レン石+白雲母+方解石+磁鉄鉱である。アクチノ閃石が定向配列することで片理を形成しており、緑簾石や褐色角閃石のポーフィロクラストを伴う。この地域の蛇紋岩メランジュ中の構造岩塊には、変成火山岩（枕状溶岩、ピロープレッチャー、火山角礫岩、水中自破碎岩）、角閃岩、マイロナイト、カタクラサイト、曹長岩、変成ハンレイ岩、蛇紋岩などが見られる。変成火山岩類は1~10mの巨大なブロックとして産する。特に枕状溶岩は、ほとんど変形を受けておらず、丸いピローローブの間を緑レン石に富む層が埋める組織を示す。鉱物組合せは、オンファス輝石+緑泥石+白雲母+緑レン石+曹長石+チタン磁鉄鉱である。ピロープレッチャーでは、枕状溶岩からピロープレッチャーへの漸移が見られ、気泡が抜けた後に方解石が充填したような組織も観察される。鉱物組合せは、ウィンチ閃石+緑泥石+緑レン石+曹長石+方解石+チタン磁鉄鉱である。水中自破碎岩では、同質の角張った岩石片がパズルのピースの様に破碎されている産状が確認でき、鉱物組合せはウィンチ閃石-バロア閃石+緑泥石+緑レン石+白雲母+曹長石+チタン磁鉄鉱である。火山角礫岩では、水中自破碎岩とは対照的な丸みを帯びた様々な岩石がブロックとして基質中に産する。鉱物組合せは、ウィンチ閃石-バロア閃石+アクチノ閃石+緑泥石+緑レン石+曹長石+チタン磁鉄鉱である。角閃岩は、1~2mの大きさのブロックとして産し、鉱物組合せは、ウィンチ閃石-バロア閃石+トレモラ閃石-アクチノ閃石+緑泥石+緑レン石+白雲母+曹長石+チタン磁鉄鉱である。マイロナイトは、1m未満の大きさのブロックとして産し、面構造が発達し、縞状の組織を呈する。また、曹長石、緑簾石の細粒多結晶集合体が確認され、角閃石のポーフィロクラストを伴う。マイロナイトの鉱物組合せは、アクチノ閃石+ツェルマク閃石+緑泥石+緑レン石+曹長石+チタン磁鉄鉱である。大部分がアクチノ閃石だが、一部 Al_2O_3 を10.40wt%含むAlに富むツェルマク閃石が確認できることから、高温でできた可能性を示唆する。カタクラサイトは、1m未満の大きさのブロックとして産し、面構造が発達する岩片の集合体であり、鉱物組合せは、アクチノ閃石+ウィンチ閃石-バロア閃石+緑泥石+緑レン石+曹長石+チタン磁鉄鉱である。変成ハンレイ岩は緑泥石の反応帯を伴う。鉱物組合せは、バロア閃石+マグネシオリーベック閃石+緑泥石+緑レン石+白雲母+曹長石+チタン磁鉄鉱である。角閃石は、多くがバロア閃石の組成を示すが、稀にマグネシオリーベック閃石を伴う。曹長岩は、拳ほどの大きさで産する。この地域の蛇紋岩メランジュは、オンファス輝石が産することや、バロア閃石-ウィンチ閃石、マグネシオリーベック閃石も見られることから緑レン石-藍閃石片岩相程度の変成作用を受けたと考えられる。

また、蛇紋岩メランジュのブロックとして方解石と赤鉄鉱に富む特異な岩石が産する。鉱物組合せは、主に単斜輝石+緑レン石+雲母+角閃石+クロム鉄鉱+曹長石+緑泥石+方解石+赤鉄鉱であり、クロム鉄鉱の割れ目、または取り囲むように単斜輝石、緑レン石、雲母、角閃石が配置する構造を示し、曹長石、方解石を除く全ての鉱物にCrが含まれる。特に、クロマイトの周囲に発達する単斜輝石、緑レン石、雲母、角閃石に多くCrが含まれる。単斜輝石では、最大6.82wt%の Cr_2O_3 を含み、核部から縁部にかけて組成累帯構造は見られない。よって拡散律速型の反応によって形成されたものではない。

キーワード：長崎変成岩、蛇紋岩メランジュ、変成火山岩

Keywords: Nagasaki Metamorphic Rocks, serpentinite melange, metavolcanic rocks

Zircon U–Pb geochronology and P–T estimation of gneisses and amphibolites from the southwestern Gyeonggi Massif, South Korea: Implication for regional middle Paleozoic metamorphism

*今山 武志¹、Oh Chang-Whan²、Jeon Jimin²、Yi Keewook³

*Takeshi Imayama¹, Chang-Whan Oh², Jimin Jeon², Keewook Yi³

1. 岡山理科大学自然科学研究所、2. 全北大学校地球環境学科、3. 韓国基礎科学研究所

1. Research Institute of Natural Science, Okayama University of Science, 2. Department of Earth and Environmental Sciences, Chonbuk National University, 3. Korea Basic Science Institute, Jeonju Center

The Hongseong area, characterized by the Permo–Triassic eclogite and high-grade rocks, in the southwestern Gyeonggi Massif, South Korea, is considered as a part of eastern extension of the Dabie–Sulu collision belt in China (e.g., Oh and Kusky, 2007). Recently, middle Paleozoic igneous and metamorphic events are also known in this area (Oh et al., 2009, 2014; Kim et al., 2008, 2014; Kwon et al., 2014). However, it is still questionable 1) whether middle Paleozoic events regionally occurred or not and 2) what kind of metamorphism occur in the southwestern Gyeonggi massif. We carried out zircon U–Pb SHRIMP ages and P–T estimation of gneisses and amphibolites in this area to constrain multiple protolith ages and metamorphic events. Migmatitic biotite gneisses in eastern Wolhyeonri complex formed during Neoproterozoic and underwent the granulite facies metamorphism (750–880 °C, 12–15 kbar) at 442–413 Ma and subsequent amphibolite facies retrograde metamorphism at 585–660 °C and 7.5–10.3 kbar. Mylonitic biotite gneiss, hornblende gneiss, and folded amphibolite also yield the metamorphic ages ranging between 429 and 420 Ma. The protoliths of several garnet amphibolites formed at 470–456 Ma due to arc magmatism, and they were also metamorphosed before 418 Ma by high pressure amphibolite facies metamorphism at ca. 625–700 °C and 13–15.5 kbar, followed by retrograde amphibolite facies metamorphism at ca. 625–700 °C and 8–9 kbar at 418–405 Ma. The SHRIMP ages obtained from a various rock type indicate that the middle Paleozoic metamorphism regionally occurred in this area. In contrast, the Paleoproterozoic augen gneisses block in the Deokjeongri gneiss complex preserve high pressure metamorphism (840–960 °C, 17–21.8 kbar) at 234–230 Ma as eclogite previously reported in this area. Regional middle Paleozoic metamorphism before high pressure Permo–Triassic metamorphism could be comparable with the middle Paleozoic Qinling orogeny in China, which were caused by the microcontinental collision before the Permo–Triassic collision between the North and South China Cratons.

キーワード：京義地塊、ジルコンU-Pb年代、古生代中期変成作用

Keywords: southwestern Gyeonggi Massif, zircon U–Pb ages, middle Paleozoic metamorphism

The numerical simulation of rigid ellipsoids rotation within Newtonian viscous matrix for the comparison with the arrangement of columnar tourmaline grains within quartz matrix in metacherts

*松村 太郎次郎¹、増田 俊明²

*Taroujiro Matumura¹, Toshiaki Masuda²

1. 静岡大学創造科学技術大学院、2. 静岡大学理学部地球科学科

1. Graduate School of Science and Technology, Shizuoka University, 2. Institute of Geosciences, Shizuoka University

We performed the numerical simulation for the rigid ellipsoids rotation within the Newtonian viscous matrix. The simulation provided the variation of the shape preferred orientation of the ellipsoids with respect to variables between the degree of non-coaxiality ($\Theta = 0^\circ-90^\circ$) and Flinn parameter ($K = 0-\infty$). We used the width and length data collected from 3621 of tourmaline grains as the shape factor of the ellipsoids, and the initial distribution pattern of the ellipsoids is assumed to be random in their orientation. Calculation results are obtained on the plane parallel to the foliation (XY-plane) and the plane vertical to the foliation in parallel with the mineral lineation (XZ-plane), because this facilitates the comparison with nature. Using the calculation result, we compared these results with the natural shape preferred orientation of tourmaline grains embedded within quartz matrix of metacherts. The comparison suggests that natural shape preferred orientation of the tourmaline grains from three metacherts correspond to a pure shear ($\Theta = 90^\circ$) and plane to constrictional strain ($K = 1-10$) with about 1-2 of finite strain.

キーワード：形態定向配列、数値シミュレーション、剛体楕円体、電気石、非共軸度

Keywords: shape preferred orientation, numerical simulation, rigid ellipsoid, tourmaline, degree of non-coaxiality

地質圧力計を用いた圧力差の再評価とその地質学的意義

Re-examination of pressure difference based on geobarometry and its geological significance

*池田 剛¹、宮崎 一博²、松浦 浩久²

*Takeshi Ikeda¹, Kazuhiro Miyazaki², Hirohisa Matsuura²

1. 九州大学大学院理学研究院地球惑星科学部門、2. 産業技術総合研究所

1. Department of Earth and Planetary Sciences, Graduate School of Science, Kyushu University, 2. Geological Survey of Japan, AIST

伝統的な地質圧力計は一般に100 MPa を越える誤差をもち、それは深さにして3.6-2.7 km の誤差に相当する。この誤差ゆえに、一つの変成帯の温度圧力構造（等圧線）を精密に決定することが困難であり、地殻進化の数値モデルの妥当性を評価するに耐える観測値を提供できない。本研究では、伝統的な地質圧力計の一般式を再評価し、同一手法で求めた試料の圧力差の誤差が圧力の絶対値の誤差よりも1桁小さいことを明らかにした。

伝統的な地質圧力計の圧力誤差は、エンタルピー変化の誤差とエントロピー変化の誤差に起因する。地殻内部で実現する温度範囲において、両者に起因する圧力誤差は同程度の値を持つ。例えば、ザクロ石-単斜輝石-斜長石-石英の反応を用いた地質圧力計の場合、エンタルピー変化の誤差に起因する圧力誤差は約120 MPa、エントロピー変化の誤差に起因する圧力誤差は727 °C で約120 MPa となる。その結果、圧力計の誤差は160 MPa となる。

これに対し、同じ地質圧力計で求めた2つの試料の条件の圧力差が持つ誤差には、エンタルピー変化の誤差に起因する誤差はなくなる。しかもエントロピー変化の誤差に乗じるのは絶対温度でなく2試料の温度差であり、有意に小さい値である。その結果、上述の例で温度差200 °C の試料間の圧力差の誤差は32 MPa となる。これは、深さにして1.2 km の差を検知できるということである。

実際の応用例として、九州北部大牟田地域に産する高温変成コンプレックスを検討する。この変成コンプレックスは白亜紀の花崗岩類と接しており、変成作用が広域なのか花崗岩による接触なのか問題となっていた。地理的に6.8 km 離れた2地点の変成条件を同一地質温度圧力計で求めたところ、圧力差が320 MPa、誤差は10 MPa であることがわかった。これは深さで11-12（誤差0.3 km）の差に相当し、変成作用時に2地点は少なくともこの距離だけ離れていたことを意味する。それが現在、6.8 km（アイソグラッドに直交する方向には2.3 km）の位置にある。間に変位の大きい断層がないことから、後退変成作用時に地殻が薄層化したことが推測される。このことは変成コンプレックスが接触変成岩でなく広域変成岩であることを示唆する。

キーワード：圧力差、地質温度圧力計、誤差

Keywords: pressure difference, geothermobarometer, uncertainty

Improving spatial resolution for quantitative microanalysis by SEM-EDS using lower accelerating voltage

*松村 里紗¹、重松 紀生²、Toy Virginia¹、針金 由美子³、Fournelle John⁴

*Risa Matsumutra¹, Norio Shigematsu², Virginia Toy¹, Yumiko Harigane³, John Fournelle⁴

1. オタゴ大学、2. 独立行政法人産業技術総合研究所、3. 独立行政法人産業技術総合研究所、4. ウィスコンシン大学マディソン校

1. University of Otago, Department of Geology, 2. Research Institute of Earthquake and Volcano Geology, National Institute of Advanced Industrial Science and Technology (AIST), 3. Research Institute of Geology and Geoinformation, Geological Survey of Japan, National Institute of Advanced Industrial Science and Technology (AIST), 4. University of Wisconsin-Madison, Department of Geosciences

Abstract

It is challenging to measure the chemical compositions of very fine-grained minerals. A method with broad utility to measure with high spatial resolution for quantitative microanalysis has not yet been established for geological materials. We are developing such a method using energy-dispersive spectrometry (EDS) in a scanning electron microscope (SEM), evaluating the effects of two corrections to improve the spatial resolution and quantitative accuracy: (1) reducing the accelerating voltage and (2) reducing the probe diameter.

We impose these corrections to counteract the fact that the interaction volume of incident electrons within a mineral expands due to electron scattering, resulting in X-rays being generated from a wider region than the incident probe diameter. It has been demonstrated that the X-ray generation volume is smaller at lower accelerating voltage, so reduction of the accelerating voltage results in an improvement of spatial resolution (e.g., Barkshire et al., 2000; Burgress et al., 2013). Reducing probe current also reduces the size of the X-ray generation volume and improves spatial resolution. Both of our corrections also result in a significant decrease in the signal intensity of the X-ray spectra.

Analyses were performed by EDS (Oxford X-Max^N 80mm² with AZtec) in a HITACHI SU-3500 SEM at the GSJ-lab in the Geological Survey of Japan, AIST. We have evaluated the spatial resolution and the signal intensity of the X-ray spectra for a range of SEM optics and EDS detector settings. A minimum accelerating voltage of 9 kV is required to quantify Fe-oxides using the signal intensity of Fe K α X-rays. Count rates of X-rays and probe currents measured through a faraday cup can be decreased by reducing accelerating voltage, spot intensity or size of aperture. The count rates of X-rays at dead times of ~45% can be processed to yield acceptable quantitative analyses. A spot intensity (condenser lens) of 63 is required to obtain a dead time of ~45% when accelerating voltage is 9 kV and aperture is No. 3 (50 μ m) in the system at the GSJ lab, by setting the longest counting time (processing time of 6) possible in AZtec. A probe current of ~0.6 nA is generated by these SEM settings.

We have so far verified the method through measurement of anhydrous and hydrous natural mineral samples. The analyses reveal that the best possible operating conditions are 9 kV accelerating voltage, spot intensity of 63, aperture No. 3, and processing time of 6. Line scans across (potentially dipping) natural mineral boundaries suggest a maximum spatial resolution of the analyses of ~1 μ m, i.e., analysis of 2 μ m diameter grains is possible. The accuracy of weight percentages of oxides is estimated as a relative difference of < 5% for MgO, Al₂O₃, SiO₂, Na₂O and K₂O and < 10% for Fe-oxides compared to

values obtained by WDS or at an accelerating voltage of 15 kV.

In future we will work to increase the accuracy of quantification of iron by obtaining proper standard spectra, and to measure spatial resolution by a combination of Monte Carlo simulations, which allow theoretical predictions of spatial resolution, a 'knife edge' technique using a sharp edge which allows measurement of lateral analytical spatial resolution, and further line scan analyses across mineral boundaries of known orientation.

Reference

Barkshire, I., et al. (2000). *Microchimica Acta*, 132(2-4), 113-128.

Burgess, S., et al. (2013). *Microscopy and Analysis*, 6, S8-S13.

キーワード : SEM-EDS システム、空間分解能、シグナル強度、微小領域の定量分析

Keywords: SEM-EDS system, spatial resolution, signal intensity, quantitative microanalysis

Evaluation of the grade of mylonitic rocks using cathodoluminescence

*菊 優太¹、河本 和郎²、西戸 裕嗣³

*Yuta Kiku¹, Kazurou Kawamoto², Hirotsugu Nishido³

1. 岡山理科大学大学院生物地球科学研究科生物地球科学専攻、2. 大鹿村中央構造線博物館、3. 岡山理科大学生物地球学部
1. Master's Program in Biosphere-Geosphere Science, Graduate School of Biosphere-Geosphere Science, Okayama University of Science Graduate School, 2. Oshika Geological Museum of Japan Median Tectonic Line, 3. Department of Biosphere-Geosphere Science, Okayama University of Science

Cathodoluminescence (CL) microscopy and spectroscopy provide useful information on existence and distribution of impurity elements related to crystal chemistry and lattice defects produced by destruction or distortion of atomic linkages with a high-spatial resolution, which should be more informative to characterize the crystal-chemical features of minerals. In this study, we have conducted to characterize CL features of the minerals in mylonitic rocks distributed in the Ryoke metamorphic belt along the Median Tectonic Line for the evaluation of mylonitization.

Mylonite, protomylonite and their source rocks (Hiji tonalite) were collected from the outcrops around an eastern part of Iida City, Nagano Prefecture. CL imaging was carried out using the Luminoscope with a cooled CCD camera. CL spectra were obtained by an SEM-CL system consisting of SEM with a grating monochromator. CL Spectral data were corrected for total instrumental response.

Color CL imaging of the mylonitic rocks shows yellow for plagioclase, blue for K-feldspar, purple to red for quartz and occasionally cream to yellow for minute zircon and apatite. In CL spectroscopy, the plagioclase with a yellow CL gives a broad band at 730-740 nm in a red region, a broad band at 570-580 nm in a yellow region and weak broad bands from 330 nm up to 430 nm in a blue region, which well correspond to the optical CL. The K-feldspar with a blue CL gives a broad band at 730-740 nm in a red region and a broad emission band at around 420 nm in a blue region. The quartz with purple to red CL gives a broad band at 640-750 nm in a red region and a broad emission band at around 390 nm in a blue region. In the quartz, the emission intensity in the blue region around 390 nm can be assigned to structural defects related to $Al^{3+}-M^{+}$ (M: Li^{+} , Na^{+} , K^{+} or H^{+}). Its intensity decreases with the progress of the mylonitization in host rocks, accompanied with its peak shift to the shorter wavelength side (higher energy side). Further more, the emission intensity at 640-750 nm in a red region due to structural defects of NBOHC and/or substitutional Fe^{3+} shows a slight increase with the mylonitization. The decrease of blue-emission intensity related to the mylonitization suggests that structural defects originally existed in the quartz for a blue-CL emission were eliminated by shear stress and/or elevated temperature during the formation of mylonite. CL characterization of the quartz could be used as an indicator for the evaluation of the mylonitization process.

キーワード：カソードルミネッセンス、マイロナイト、圧砕岩類

Keywords: Cathodoluminescence, Mylonite, Mylonitic rocks